Origins of Stereoselectivity in the Diels−Alder Addition of Chiral Hydroxyalkyl Vinyl Ketones to Cyclopentadiene: A Quantitative Computational Study†

Snezhana M. Bakalova and Jose Kaneti*

Institute of Organic Chemistry with Centre of Phytochemistry, Bulgarian Academy of Sciences, G. Bonchev str., Block 9, 1113 Sofia, Bulgaria

Received: April 28, 2008; Revised Manuscript Received: May 26, 2008

Modest basis set level MP2/6-31G(d,p) calculations on the Diels−Alder addition of *S*-1-alkyl-1-hydroxy-but-3-en-2-ones (1-hydroxy-1-alkyl methyl vinyl ketones) to cyclopentadiene correctly reproduce the trends in known experimental endo/exo and diastereoface selectivity. B3LYP theoretical results at the same or significantly higher basis set level, on the other hand, do not satisfactorily model observed endo/exo selectivities and are thus unsuitable for quantitative studies. The same is valid also with regard to subtle effects originating from, for example, conformational distributions of reactants. The latter shortcomings are not alleviated by the fact that observed diastereoface selectivities are well-reproduced by DFT calculations. Quantitative computational studies of large cycloaddition systems would require higher basis sets and better account for electron correlation than MP2, such as, for example, CCSD. Presently, however, with 30 or more non-hydrogen atoms, these computations are hardly feasible. We present quantitatively correct stereochemical predictions using a hybrid layered ONIOM computational approach, including the chiral carbon atom and the intramolecular hydrogen bond into a higher level, MP2/6-311G(d,p) or CCSD/6-311G(d,p), layer. Significant computational economy is achieved by taking account of surrounding bulky (alkyl) residues at 6-31G(d) in a low HF theoretical level layer. We conclude that theoretical calculations based on explicit correlated MO treatment of the reaction site are sufficiently reliable for the prediction of both endo/exo and diastereoface selectivity of Diels−Alder addition reactions. This is in line with the understanding of endo/exo selectivity originating from dynamic electron correlation effects of interacting π fragments and diastereofacial selectivity originating from steric interactions of fragments outside of the Diels−Alder reaction site.

Introduction

Chiral induction in Diels−Alder (DA) additions is most conveniently achieved via the attachment of various chiral auxiliaries to corresponding dienophiles and/or dienes. The derivatives of acrylic acid with the common acryloyl fragment **1**, Scheme 1, are among the simplest dienophiles studied extensively in asymmetric reactions with dienes.[1–5] For this purpose, synthetically versatile auxiliaries have been attached to the acryloyl carbon through an O or N spacer to produce chiral acrylate esters **2**[1] or acrylamides **3**,[6] respectively, Scheme 1. Stronger asymmetric induction has been achieved, however, with the chiral carbon center directly attached to the acryloyl carbon atom, that is, with chiral alkyl vinyl ketones **4**,[2,3] Scheme 1. Experiments with specifically designed[2,3] ketone dienophiles **5a** and **5b** proceed at room temperature with the expected higher endo/exo selectivity and, in particular, π-facial diastereoselectivity of up to 100/1,[2,3] that is, significantly enhanced relative to the moderate selectivities of ∼4/1 with acrylates or acrylamides.[1] This stronger asymmetric induction has been attributed at least in part to the catalytic assistance of the intramolecular hydrogen bond of the designed dienophiles **5**.[2,3]

A vast number of computational studies of DA additions has frequently led to controversial results regarding stereoselectivity, resulting in essentially little progress in its understanding since the publication of the Woodward−Hoffmann rules.[4,5] To the contrary, mechanistic aspects of the DA reaction have been treated with considerably greater success[6–9] to show, in the majority of cases, a concerted, although asynchronous, mechanism of the cycloaddition, with the alternative stepwise diradical cases usually regarded as exceptions. The concerted DA mechanism can thus be considered generally accepted, and a standard set of pericyclic hydrocarbon reactions for the benchmarking of adequate state-of-the-art high-level computational methods has been developed.[10] For example, the complete basis set multicoefficient correlated CBS-QB3 method reproduces activation enthalpies and entropies, reaction heats, and transition-state geometries closest to experiment.[10] Another recent computational effort directed toward the elucidation of DA stereoselectivity with the chiral acrylate ester of ethyl-*S*-lactate (**2**: R* = ethoxy-*S*-lactyl, Scheme 1)[11] has shown that modest level MP2/6-31G(d,p) calculations correctly reproduce the experimentally determined stereoselectivities in that specific case,[12] while the B3LYP/6-31G(d,p) treatment fails in the prediction of the endo/exo selectivity.[11] Endo/exo selectivity of furan DA additions has been studied at the highest level so far, CCSD(T)/aug-cc-pVDZ//MP2/6-31+G(d).[13] The latter study concludes that endo/exo selectivity is the result of interplay of several factors, requiring elaborate analysis of correlation energy and solvent effects, while quite outside of the addressable scope of concepts like molecular mechanics-like electrostatic forces[14] or secondary orbital interactions.[15] The mentioned high level of modeling is regrettably quite out of reach for Diels−Alder additions of larger and/or heteroatomic reactants and even more so with catalyzed DA reactions by, for example, Lewis acids or chiral auxiliary agents. Due to the obvious need of compu-

† Part of the "Sason S. Shaik Festschrift".

* To whom correspondence should be addressed. E-mail: kaneti@orgchm.bas.bg.

10.1021/jp803701y CCC: $40.75
Published on Web 07/19/2008

SCHEME 1: Acryloyl Dienophiles[a]

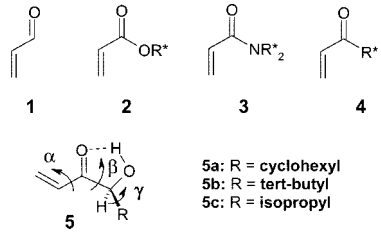

[a] R* stands for chiral "auxiliaries"; α, *β*, and *γ* are the conformational degrees of freedom, discussed with regard to reaction selectivity hereafter.

tationally more feasible approaches, we attempt to validate a computationally less demanding while still sufficiently rigorous methodology, ONIOM,[16] for prediction of Diels−Alder stereoselectivity on the experimental example of chiral hydroxyalkyl vinyl ketones **5** with cyclopentadiene, **CPD**.[2,3] A related layered IMOMO study of an enantioselective benzoin condensation has been reported recently.[17] A full ONIOM approach for the study of enantioselective deprotonation has also been reported.[18] Closely related to the present study are an early MP3[19] and a recent QM/MM investigation of the addition of methyl vinyl ketone (**MVK**) and other dienophiles to **CPD**, including reaction acceleration in increasingly polar solvents.[20]

The challenge to any computational study of stereoselectivity is offered by the critical theoretical values of computed Gibbs free activation energy differences $\Delta\Delta G^{\ddagger}$ between respective diastereoisomeric transition structures. For a reaction with relatively low kinetic stereoselectivity, for example, 3/2, the corresponding $\Delta\Delta G^{\ddagger}$ is roughly 0.25 kcal·mol^{-1} at 300 K, that is, well beyond the limit of precision of state-of-the-art molecular quantum mechanics calculations of individual organic molecules.[13] With DA reactions, one is virtually confronted with even lower selectivities, which does indeed impose heavy demands on the quality of any theoretical approach. However, in the case of stereoselective (and enantioselective) reactions, one has to deal with isomeric molecules and/or transition structures with strictly reduced structural differences and topologically identical fragments, which justifies the expectation for favorable cancelation of (nearly identical) computational errors and, hopefully, reliable theoretical values for Gibbs free activation energy differences down to 0.5 kcal·mol^{-1} or even less. Encouraging computational examples of relative $\Delta\Delta G^{\ddagger}$ have been reported in the recent QM/MM study of methyl vinyl ketone, **MVK**, to cyclopentadiene, **CPD**, in several solvents.[20] We can thus expect to quantitatively reproduce stereoselectivity trends and analyze origins of stereoselectivity by computations with references to reliable experimental data.

Computational Details

Geometries of studied reactants, chiral hydroxyalkyl ketones **5** and cyclopentadiene, and transition structures, TSs, of their Diels−Alder addition are completely optimized by default procedures of Gaussian 03[21] at either the frozen core MP2 or the B3LYP levels of theory, using several basis sets ranging from 6-31G(d) up to 6-311+G(2d,p).[22] Stationary structures on the studied potential energy surfaces are verified by vibrational analysis, requiring positive definite second energy derivative matrices for the minima or a unique imaginary vibrational mode for the TSs. Thermochemical corrections to the total energy at 298.15 K of all studied molecular species—reactants, TSs, and products—are calculated on the basis of unscaled vibrational frequencies. Intrinsic reaction coordinate following,[23] IRC, calculations are used to distinguish reaction mechanisms out of the two possible alternatives, concerted or stepwise. Single-point MP2 and B3LYP total energy calculations at triple-ζ-quality basis set levels are done with either Gaussian 03 or GAMESS-US.[24] Higher levels of dynamic electron correlation are achieved in hybrid ONIOM[16,25] calculations. In the latter evaluation of electron correlation contributions to studied reaction energetics, we use a correlated, for example, MP2, layer with either 6-31G(d,p) or 6-311G(d,p) basis sets as the "model" part of the reacting molecules, ONIOM-MP2,[25] which includes all molecular fragments essential to the asymmetric induction. We consider as such the reacting *π* fragments, the chiral carbon atom, and the catalytic hydrogen bond. Another "low" level part uses HF/6-31G(d) for the remaining molecular fragments, as well as for the real system. Better account for electron correlation corrections is achieved using a high-level CCSD/6-311G(d,p)[26] model layer while preserving the low level HF/6-31G(d) layer for single-point ONIOM-CCSD calculations at the corresponding optimized ONIOM-MP2 TS geometries. The selection of layer separations is described in detail in the Discussion. Molecular energy values in the used hybrid ONIOM scheme are defined as[16,25]

$$E^{\mathrm{ONIOM}} = E^{\mathrm{model,high}} + E^{\mathrm{real,low}} - E^{\mathrm{model,low}} \qquad (1)$$

where model is the part of molecular system deemed essential for the reaction and real is the entire reacting system. High and low refer to used levels of calculation in the respective layers.

To account for solvent effects on the geometries and relative energies of studied Diels−Alder TSs, we use solvent model calculations by the self-consistent continuum method[27] in its conductor-like approximation, CPCM.[28] The used solvent is toluene, as in the experiments.[2]

Results and Discussion

Conformational Aspects of the Reaction. DA cyclizations are processes with large negative entropy of activation up to −45 cal·mol^{-1}·K^{-1},[10,29] which in general changes insignificantly[10,19,29] with substituents to either diene or dienophile. Therefore, possible changes of entropic contributions to computed Gibbs activation free energies of **CPD** addition would only be expected from conformational changes in reactants, for example, studied dienophiles **5**, Scheme 1. Note that these entropic contributions can be significantly larger than the mandatory precision of better than 0.5 kcal·mol^{-1} for stereochemical computations. Therefore, account for conformational changes and hydrogen bonding in DA reactants and/or TSs, including nontraditional C−H···O bonds, has been shown to reconcile some discrepancies between experimental secondary kinetic isotope effects and theoretical computations on Lewis-acid-catalyzed DA additions.[30] In view of the crucial importance of minute activation free-energy differences $\Delta\Delta G^{\ddagger}$ to corresponding kinetic diastereoselectivity ratios, we pay specific attention to conformational properties of reactants and TSs. This is also mandatory in view of the Curtin−Hammett principle,[31] attributing largest product contributions from lowest free activation energy profiles irrespective of relative reactant populations in the case of fast interconversion of reactant conformers. In the opposite case of slow conformational interconversion of reactants, one may expect certain propagation of rotational populations of reactants to TSs and further to the products, or "conformational memory". Specific cases of the latter phenomenon have even been termed "stereochemical transcription".[32] Once again, as stereoselectivity is particularly sensitive to small relative differences of activation free energies

$\Delta\Delta G^{\ddagger}$, all mentioned contributions have to be specifically accounted for in a quantitative theoretical study.

Scheme 1 shows the internal rotations in dienophiles **5** with virtually important entropic contributions. For the model dienophile *S*-1-hydroxy-1-isopropyl methyl vinyl ketone, **5c**, the internal rotation α about the (C═)C−C(═O) bond has, at the modest MP2/6-31G(d,p) level of calculation, two relatively low rotational barriers of 4.3 and 5.1 kcal·mol^{-1}. These values are lower than the published barrier for acrolein *s-cis*−*s-trans* isomerization, 8.9 kcal·mol^{-1} at the HF/6-31G(d)//3-21G level.[33] The calculated population of the most stable *s-cis* hydrogen-bonded rotamer prevails over the *s-trans* hydrogen-bonded one by 7.4/1, as shown by calculated MP2(fc)/6-31G(d,p) free-energy differences. This preference for the *s-cis* rather than the *s-trans* isomer[19] of the dienophile contradicts experiments with parent methyl vinyl ketone[34] but corroborates earlier theoretical expectations favoring *s-cis* conformers for **MVK**.[19]

Limitation of the rotational degree of freedom β with respect to the (HO)C*−C(═O) bond should lead by design to relatively large free-energy differences and, consequently, to a single dominant hydrogen-bonded isomer out of the three possible rotamers,[2,3] Scheme 1. Calculated MP2/6-31G(d,p) free-energy barrier to this rotation, accompanied by hydrogen bond breaking, is however only 5.7 kcal·mol^{-1}, that is, could hardly be considered an indication of "freezing of the free rotation" suggested in the dienophile design.[2] The latter value cannot be a convincing argument in favor of amplified stereoselectivity by the intramolecular hydrogen bond in hydroxyalkyl vinyl ketones **5a** and **5b** either. Masamune et al.[2] have apparently solved the problem experimentally by silylation of the hydroxyl group,[2,3] thereby reducing the selectivity to insignificant. However, the reported experimental result is inconclusive insofar it can well be due to either disruption of the apparently weak OH···O═C bond or to the much greater steric bulk of the silyl group, or both.

To refine conformational energy predictions, we use single-point MP2/6-311++G(2d,p)//MP2/6-31G(d,p) calculations aiming at a better account of hydrogen bonding and more reliable relative energies of **5c** conformers. At this higher level, the *s-cis* and *s-trans* hydrogen-bonded conformers become even closer in energy, while the predicted β rotation barrier between the hydrogen-bonded *s-cis* and the more stable of two non-hydrogen-bonded *s-cis* conformers increases to ∼12 kcal·mol^{-1}. The latter energy value can be considered sufficient corroboration of the experimental deduction of significantly hindered rotation and thereby effective "hardwiring" of the chiral carbon atom to the cycloaddition reaction site,[2] responsible for the observed high asymmetric induction and stereoselectivity, as well as for a certain extent of intramolecular catalysis.

One more degree of conformational freedom, and virtually a source of substantial entropic contributions to the theoretical Gibbs free activation energies, is represented by the rotation γ about the (O═)C−C*−C−C bond, Scheme 1. The latter dihedral angle determines the conformational arrangement of the 1-alkyl substituent at the chiral carbon atom with respect to the approximate plane of the dienophile system including the five-membered hydrogen-bonded cycle. A conformational scan for **5c** reveals three minima, with the preferred conformer having a methyl substituent staggered between the C═O and HO substituents at the chiral carbon and the hydrogen atom pointing toward the acceptor C═C bond of the dienophile, Scheme 2. MP2/6-31G(d,p) geometry optimizations of the located conformational minima of **5c** reveal populations of ∼3 and 2% for the two less stable *s-cis* conformers. Among the rotational minima of *s-cis* **5c**, the H-staggered-between-C═O···HO rotamer is the least stable one, though still having a non-negligible population center, Scheme 2.

SCHEME 2: Newman Projections of Alkyl Rotational Minima with Respect to Angle γ of 1-*S*-hydroxyalkyl Vinyl Ketones 5, with the Chiral Carbon (Circle) in the Background[a]

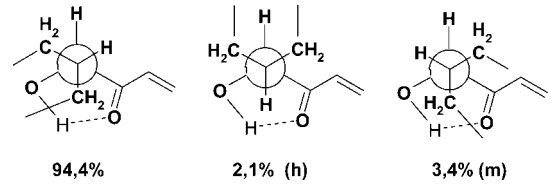

[a] The percentage of gas-phase MP2/6-31G(d,p) populations at 300 K is shown for rotational isomers of *s-cis* **5c**.

SCHEME 3: Diastereoisomeric Products of the DA Addition of *s-cis* 1-Hydroxyalkyl (R*) Vinyl Ketone and Cyclopentadiene

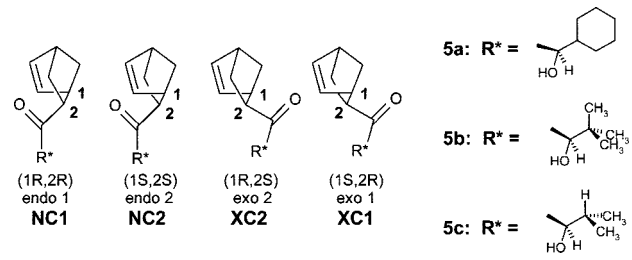

The same conformational situation should evidently occur also with **5a** and prompts the location of reaction TSs arising from at least two border-case conformers of dienophiles **5a** and **5c**. Thus, we would be able to assess quantitatively the significance of steric interactions between the bulky alkyl substituent and the dienophile C═C bond to the energetics of corresponding DA TSs.

With the chiral *S*-carbon "hardwired" in the dienophile and the small substituent (hydrogen) at the next carbon atom also pointing toward the dienophilic C═C double bond and the incoming diene, one should expect a preferred re-attack on the prochiral dienophile carbon atom C_2, that is, a preference for 2*S*-diastereoisomeric adducts, Scheme 3. This line of reasoning is in line with earlier considerations of Prelog,[35] Cram,[36] Walborsky[37] and Helmchen[1] regarding the expected configuration of preferred diastereoisomeric products.

With the assumption that cycloaddition TSs are more or less product-like, Scheme 3 also shows the configuration of four possible TSs arising from the addition of the *s-cis* isomer of a dienophile **5** to **CPD**. Another four products, respectively TSs, can evidently derive from the *s-trans* isomers of corresponding dienophiles. Thus, technically, the problem at hand is the location of eight hydrogen-bonded diastereoisomeric TSs and the calculation of their activation free energies, $\Delta\Delta G^{\ddagger}$, relative to the kinetically most rapidly forming stereoisomer. To distinguish between the studied TSs, we use the notation of TS diastereoisomers elaborated recently by one of us with **N** and **X** denoting endo and exo and **C** and **T** denoting *s-cis* and *s-trans*, respectively.[11] We consider in detail the extent to which computation models reproduce the designed experimental DA stereoselectivity in the attempt to reveal its underlying origins in terms of electronic structure theory.

Computed activation-free-energy differences predict the corresponding kinetic stereoselectivities on the basis of the simple Arrhenius equation

$$\Delta G_0^{\ddagger} - \Delta G_i^{\ddagger} = -RT \cdot \ln(k_0/k_i) \quad (2)$$

where $\Delta G_0^{\ddagger}$and k_0 are the calculated free activation energy and reaction rate constant of the favored stereoisomer and $\Delta G_i^{\ddagger}$ and k_i refer to the remaining stereoisomers.

DFT Results in the Gas Phase. Routine B3LYP/6-31G(d) calculations of hydroxy-**MVK 5** to **CPD** give rather disappointing results in terms of calculated relative activaton free energies of located TSs. For example, for the addition of **5a** to **CPD** reversed to experiment, endo/exo selectivity in favor of the exo diastereoisomer is computed. The picture is corrected slightly by B3LYP/6-31G(d,p) calculations, by means of which an endo/exo ratio of products of 2/1, still much lower than experiment, ∼7/1,[2] is obtained. Therefore, as a reasonable compromise between computational effort and expected stereochemical result, we carry out B3LYP optimizations using the rather large 6-311+G(2d,p) basis for the gas-phase reactions of the smaller model dienophile **5c** and **CPD**.

Calculated B3LYP/6-311+G(2d,p) activation ($\Delta E^{\ddagger}$) and activation free energies ($\Delta E^{\ddagger} + \Delta G^{\ddagger}$) of the TSs in the addition of **5c** and **CPD** relative to the reactants are given in Table 1. $\Delta E^{\ddagger}$ values are relatively low, as indicated earlier for calculated DFT activation energies for electrocyclic reactions, while free activation energies $\Delta E^{\ddagger} + \Delta G^{\ddagger}$ are about twice as high, in line with the known large activation entropies of DA additions. Compared to earlier MP3/6-31G(d) free activation energies of **MVK** addition to **CPD**, 30−35 kcal·mol^{-1},[19] present B3LYP values are within the same range of magnitude.

Located TSs on the B3LYP/6-311G(d,p) potential surface, Figure 1, are rather dissymmetrical in the mechanistic sense, with lengths of the forming C···C bonds of $\sim d_1 = 1.96$ Å for the shorter and d_2 between 2.63 and 2.70 Å for the longer one, that is, $\Delta d \sim 0.7$ Å or $d_2/d_1 \sim 1.35$. Further, we use the computed second energy derivative matrices at the verified transition structures to follow the corresponding IRC and thereby rigorously analyze the reaction mechanism.[23] The unimodal IRC energy profiles show that the located TSs, Figure 1, correspond to a concerted though asynchronous mechanism. Indeed, our attempts to locate computationally any singlet TS or intermediate corresponding to stepwise addition failed at both DFT and 12 × 12 MCSCF/6-311G(d,p)[25] gas-phase levels of computation.

Our highest-level DFT calculations, B3LYP/6-311+G(2d,p) for the reaction of **5c** and **CPD**, show that the contribution of *s-trans* isomers of the dienophile to the addition products is completely negligible, Table 1. The same result was found in earlier MP3/6-31G(d) calculations for the addition of **MVK** to **CPD**.[19] Calculations on the possible alkyl rotation

TABLE 1: B3LYP Activation Energies for the Addition of 5c to CPD in the Gas Phase and in Toluene Solution ($\Delta E^{\ddagger}$ Total, $\Delta E^{\ddagger} + \Delta G^{\ddagger}$ Total Plus Gibbs Free-Energy Correction at 298.15 K, and $\Delta\Delta G^{\ddagger}$ − Relative Free Activation Energy) Relative to the Most Stable (*s-cis*) CH_3-Staggered-between-OH···O(=C) Conformer with Fully Optimized Gas-Phase B3LYP/6-311+G(2d,p) TSs, Single-Point CPCM/B3LYP/6-311+G(2d,p)//B3LYP/6-311+G(2d,p), and Fully Optimized CPCM/B3LYP/6-311G(d,p) TSs[a]

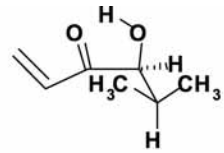

TS		6-311+G(2d,p)$_{vac}$	SP/CPCM/6-311+G(2d,p)	CPCM/6-311G(d,p)
NC1	ΔE‡	18.51	18.67	17.44
	ΔE‡+ΔG‡	33.97	34.00	32.72
	ΔΔG‡	2.4 1.3%	2.8 0.7%	2.65 0.9%
NC2	ΔE‡	16.68	16.61	15.23
	ΔE‡+ΔG‡	31.55	31.23	30.07
	ΔΔG‡	0.0 69.3%	0.0 78%	0.0 77%
XC1	ΔE‡	18.39	19.14	17.44
	ΔE+ΔG‡	33.94	34.55	32.98
	ΔΔG‡	2.4 1.3%	3.3 0.3%	2.9 0.6%
XC2	ΔE‡	16.91	17.06	15.55
	ΔE‡+ΔG‡	32.09	32.01	30.84
	ΔΔG‡	0.54 28.2%	0.78 21%	0.77 21%
NT1	ΔE‡	20.76	20.46	19.29
	ΔE‡+ΔG‡	36.52	36.04	35.02
	ΔΔG‡	5.0	4.8	4.9
NT2	ΔE‡	34.14	24.34	28.85
	ΔE‡+ΔG‡	49.46	40.37	45.75
	ΔΔG‡	17.9	9.1	15.7
XT1	ΔE‡	22.16	22.05	20.91
	ΔE‡+ΔG‡	37.27	36.91	35.75
	ΔΔG‡	5.7	5.7	6.3
XT2	ΔE‡	25.85	26.04	24.97
	ΔE‡+ΔG‡	41.75	41.88	40.88
	ΔΔG‡	10.2	10.6	10.8

[a] All energies are in kcal·mol^{-1}. The respective kinetic product percentage distributions are given also for *s-cis* isomers. For the designations of stereoisomers, see Scheme 3.

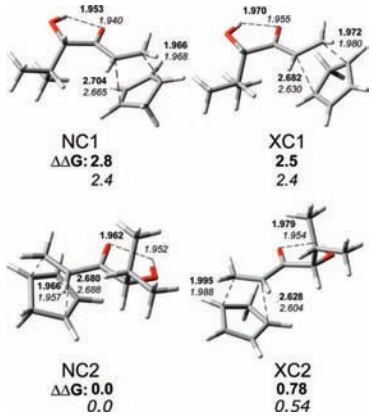

Figure 1. Optimized B3LYP TSs and relative activation free energies $\Delta\Delta G^{\ddagger}$ for the addition of the most stable rotamer of **5c** to **CPD** in vacuum, 6-311+G(2d,p), italic, and in toluene solution, 6-311G(d,p), boldface. Forming bond lengths are given in Å, and $\Delta\Delta G^{\ddagger}$ is in kcal·mol^{-1}.

conformers of preferred TSs, **NC2** and **XC2**, give differences in calculated free activation energies for the respective reaction paths, indicating almost negligible contributions to the reaction products in the range of ~1%. For this reason, we only consider hereafter the four lowest endo and exo B3LYP TSs arising in the reactions of **CPD** with *s-cis* dienophiles **5a** and **5b**, Table 2, leaving out both *s-trans* and alkyl rotational isomers. The predicted endo/exo preference of **NC2** vs **XC2** products from **5a** and **5b** remains low, ~2.5/1, which is significantly lower than the experimental ratio. For the addition to the other face of the dienophile, the calculated **NC1** versus **XC1** endo/exo selectivity vanishes, Table 1, whereas experiments give 8/1 for **5a**.[2] Only the predicted endo diastereoface selectivity by B3LYP/6-311+G(2d,p) is closer to experiment, 47/1 versus 100/1.

In summary, as related to earlier MP3 calculations on the reaction of unsubstituted **MVK**,[19] the endo/exo selectivities resulting from discussed DFT calculations are about the same but significantly lower than those found experimentally for the additions of **5a** and **5b** to **CPD**.[2]

MP2 Results in the Gas Phase. Next, we reoptimize the diastereoisomeric TSs for the addition of the model dienophile **5c** by MP2/6-31G(d,p) calculations. We consider the TSs for the addition of **CPD** to three hydrogen-bonded conformers, that is, including all isomers originating from rotation γ around the C*−C bond, Schemes 1 and 2, in order to estimate the range of the computed reaction thermodynamic parameters. Table 3 summarizes the MP2 results for 16 TSs arising from the most stable CH_3-staggered-between-OH···O(=C) conformer of **5c** and the least stable H-staggered-between-OH···O(=C) conformer of **5c**(h), as well as the 4 TSs arising from the *s-cis* **5c**(m) rotational isomer.

Calculated MP2 activation free energies are significantly lower than DFT values discussed in the previous section. These values are also lower than reported MP2/6-31G(d) activation energies for the addition of **MVK** to **CPD** on the order of 2 kcal·mol^{-1} and even more so than MP3/6-31G(d) activation free energies on the order of 16 kcal·mol^{-1}.[19] On the basis of the known deficiency of MP2 in overestimating the dynamic correlation energy, along with the correct prediction of stereoselectivity, we deduce that computed MP2/6-31G(d) activation energies are systematically in error by ~−12 kcal·mol^{-1}. In the present DA reaction, calculated values of $\Delta E^{\ddagger} + \Delta G^{\ddagger}$ indicate a considerably higher reactivity of the studied hydroxy-**MVK** than unsubstituted **MVK** itself.[19] In other words, not only does the intramolecular hydrogen bond of hydroxyketone **5** enhance stereoselectivity, but it has a significant catalytic effect of ~3 − 4 kcal·mol^{-1} on the addition reaction as well. This is an expected result as Lewis acids, and H^+ is no exception, do indeed have a catalytic effect on DA additions of acrylates.

The MP2 energy differences between TSs arising from *s-cis* and *s-trans* dienophile, Table 3, are significantly amplified in favor of the *s-cis* products, related to corresponding DFT values, Table 1. More interesting and indeed much more significant are the computational predictions of diastereoselectivity, in particular endo/exo. In contrast to DFT results, MP2/6-31G(d,p) calculations on the addition of **5c** and **CPD** predict a clear kinetic preference for endo over exo adducts, in line with reported experiments.[2,3] Calculated MP2 product percentage distributions further show that **NC2** and **XC2** are dominating, and the following discussion of stereoselectivity will be focused mainly on the ratio of these two diastereosiomers.

The calculated MP2/6-311+G(2d,p)//MP2/6-31G(d,p) activation-free-energy differences **NC2** − **XC2** for the reaction of the most stable (O=)C−C*−C_{alkyl}−C conformer of *s-cis* **5c** and **CPD** predict endo/exo selectivity of ~5.3/1, Table 3, which is still somewhat low relative to experiments.[2] The predicted contribution from *s-trans* **5c** remains practically unchanged at the two MP2 basis set computational levels, ~1% from the **NT1** isomer, Table 3. This is anyway about the experimental limit of detection.[2] An additional factor disfavoring the addition to *s-trans* vinyl ketones **5** is the steric repulsion of diene and the bulky alkyl substituent, reaching its extreme in the failure of **XT2** optimization of **5c**(h), Table 3.

A significant detail of MP2 optimizations at the 6-311G(d,p) and higher basis set levels is that electronic activation energies decrease to negative, Table 3. As discussed above and noted in earlier calculations of the **MVK** reaction with **CPD**,[19] this effect stems from overestimation of dynamic correlation effects by MP2 and should indeed increase with larger basis sets. Previously, this purely computational effect has apparently been corrected by higher-level MP3 calculations.[19] Specifically, bearing in mind also the large negative entropy of DA cycloadditions,[10,19] their free activation energy clearly cannot be approximated as MP2 electronic activation energy.

Theoretical selectivities for **5a** (Table 4) compare favorably with available experimental data at room temperature. The predicted endo-diastereoface selectivity (**NC2/NC1**) is ~17/1, which is close to the experimental value, 13/1. For the exo-diastereoface selectivity **XC2/XC1**, we obtain a calculated ratio of ~14/1, which is also close to the experimentally determined exo-diastereofacial selectivity of 8/1.[2] Particularly gratifying is the finding that endo-diastereoface selectivity should be higher than its exo counterpart, as also observed in the experiment. The generalized experimental endo/exo selectivity for **5a**, (**NC2** + **NC1**)/(**XC2** + **XC1**) is calculated to be 4.3/1, while the experimental value is 8/1.[2]

For **5b**, experiments have shown diastereoface selectivity of 23/1 at room temperature for the endo products, whereas its value has not been determined for the exo products.[2] The overall endo/exo selectivity has been determined at ~6/1 at room temperature and up to 8/1 at low temperature. Computed diastereoface selectivities for **5b**, Table 4, are in all cases higher than 100/1, while the room-temperature value for the **NC2/XC2** selectivity ratio is ~5/1, close to experiment.[2]

With **5a** and **5c**, we explicitly consider the conformational contributions of possible alkyl rotational dienophile conformers, Tables 3 and 4. The results show that products originating from

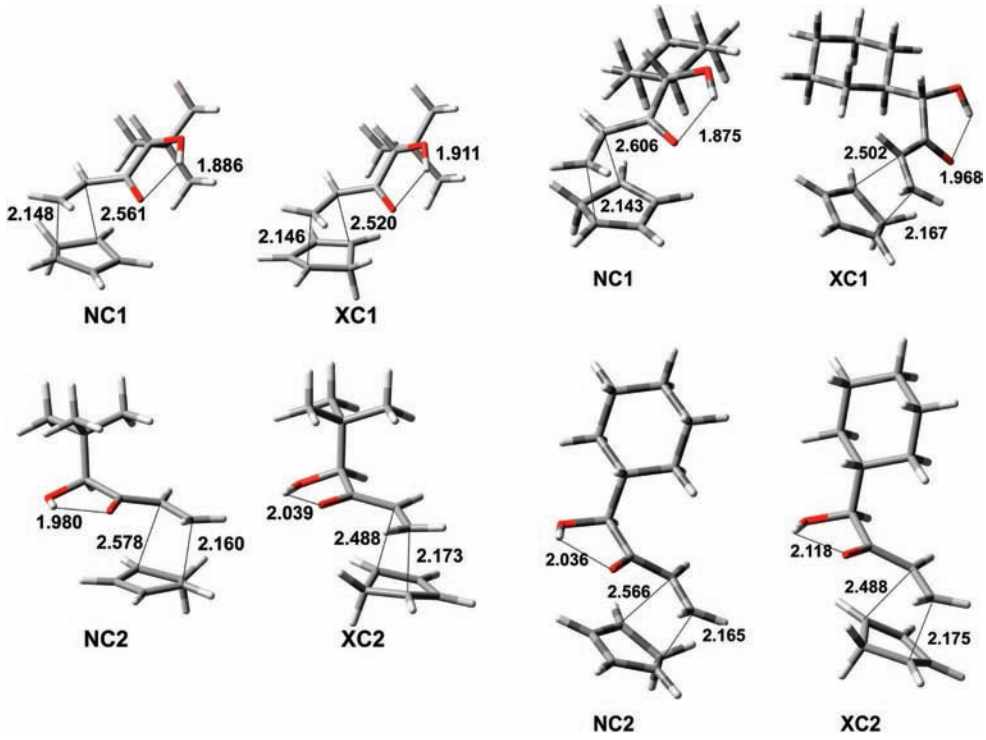

Figure 2. Selected structural parameters of TSs for the additions of **5b** (left) and **5a**(h) (right) (a minor rotamer, see Table 3 and also cf. Figure 6) to **CPD**, MP2/6-31G(d,p). Forming C···C bonds and the catalytic hydrogen bond are indicated by thin lines, with lengths given in Å; $\Delta d < 0.5$ Å in all cases, that is, the TSs are more "synchronous" than their corresponding DFT counterparts.

TABLE 2: B3LYP Activation (Total Electronic $\Delta E^{\ddagger}$ and Gibbs Free $\Delta E^{\ddagger} + \Delta G^{\ddagger}$; relative $\Delta\Delta G^{\ddagger}$) Energies for TSs of the Addition of 5b and 5a to CPD in the Gas Phase[a]

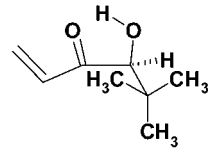

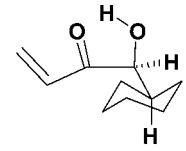

TS		6-311G(2d,p)	SP/CPCM/B3LYP/6-311G(d,p)	6-311G(2d,p)
NC1	$\Delta E^{\ddagger}$	18.32	27.61	17.65
	$\Delta E^{\ddagger}+\Delta G^{\ddagger}$	33.57		33.17
	$\Delta\Delta G^{\ddagger}$	3.8 0.1%	3.6 0.1%	2.36 1.4%
NC2	$\Delta E^{\ddagger}$	14.82	23.98	15.59
	$\Delta E^{\ddagger}+\Delta G^{\ddagger}$	29.76		30.83
	$\Delta\Delta G^{\ddagger}$	0.0 69.5%	0.0 62%	0.0 68.6%
XC1	$\Delta E^{\ddagger}$	17.93	27.27	19.91
	$\Delta E^{\ddagger}+\Delta G^{\ddagger}$	33.44		35.71
	$\Delta\Delta G^{\ddagger}$	3.7 0.1%	3.3 0.2%	4.9 0.02%
XC2	$\Delta E^{\ddagger}$	15.19	24.30	15.87
	$\Delta E^{\ddagger}+\Delta G^{\ddagger}$	30.26		31.32
	$\Delta\Delta G^{\ddagger}$	0.5 30.2%	0.3 37.6%	0.51 30%

[a] Solution results in toluene are given for **5b**, single-point CPCM/B3LYP/6-311G(d,p) TSs. Relative total electronic and free-energy differences are in kcal·mol^{-1}. The respective kinetic product percentage distributions are given also for each entry.

the minor conformers should only have minimal impact over the product selectivity. In fact, calculation of overall product stereoselectivity shows that the account for contributions from the minor reactant conformer **5a**(h) should slightly increase diastereoface selectivity, while leaving the endo/exo selectivity practically intact.

MP2/6-31G(d,p) calculations of vinyl ketone **5** additions to **CPD**, as reported here, apparently support the recent deductions of importance of dynamic electron correlation effects in DA, in particular endo/exo, selectivity.[13] MP2/6-31G(d,p) endo/exo selectivities are higher than best B3LYP values, although still lower than experiment. Both MP2/6-31G(d,p) calculations and significantly higher basis set B3LYP calculations show higher diastereoface selectivity for **5b** than that for **5a**, Table 2, as found also by experiment.[2,3] The logical development of this study would require higher basis set MP2 or better correlated calculations of the modeled reaction. With molecules of the present size, however, the reported MP2/6-31G(d,p) calculations

TABLE 3: MP2 Gas-Phase and Solution Activation Energies for TSs Optimized at the MP2/6-31G(d,p) Gas-Phase Level, Single-Point MP2/6-311+G(2d,p)//MP2/6-31G(d,p) Gas-Phase Level, and Single-Point MP2/6-311G(d,p)//MP2/6-31G(d,p) in Toluene CPCM[25] (Total Electronic Energies $\Delta E^{\ddagger}$ with Free-Energy Corrections $E^{\ddagger} + \Delta G^{\ddagger}$, As Well As Relative Activation Free Energies $\Delta\Delta G^{\ddagger}$) for the Addition of 5c to Cyclopentadiene at 298 K[a]

		5c			**5c**(h)		**5c**(m)
TS		6-31G(d,p)	6-311+G(2d,p)	CPCM	6-31G(d,p)	6-311+G(2d,p)	6-31G(d,p)
NC1	$E^{\ddagger}$	2.35	−1.0	0.57	2.93	−0.47	2.95
	$E^{\ddagger} + \Delta G^{\ddagger}$	18.23			18.67		22.26
	$\Delta\Delta G^{\ddagger}$	2.4, 1.5%	1.7, 4.6%	1.9, 3.1%	2.8	2.25	8.4
NC2	$E^{\ddagger}$	0.56	−2.72	−1.32	−0.69	−3.57	−0.33
	$E^{\ddagger} + \Delta G^{\ddagger}$	15.84			14.89		15.39
	$\Delta\Delta G^{\ddagger}$	0.0, 80.5%	0.0, 78.5%	0.0, 75.9%	**−0.95**	**−0.85**	1.5
XC1	$E^{\ddagger}$	2.40	−0.4	1.04	2.87	−0.09	3.11
	$E^{\ddagger} + \Delta G^{\ddagger}$	18.57			18.95		19.17
	$\Delta\Delta G^{\ddagger}$	2.73, 0.8%	2.3, 1.7%	2.4, 1.3%	3.4	2.6	5.3
XC2	$E^{\ddagger}$	1.26	−1.7	−0.53	−0.15	−2.69	1.53
	$E^{\ddagger} + \Delta G^{\ddagger}$	16.77			15.59		16.11
	$\Delta\Delta G^{\ddagger}$	0.93, 17.1%	1.02, 14.1%	0.8, 19.7%	**−0.25**	0.0	2.3
NT1	$E^{\ddagger}$	2.51	−0.6	4.82	1.69	−10.48	
	$E^{\ddagger} + \Delta G$ ‡	18.20			17.62		
	$\Delta\Delta G^{\ddagger}$	2.8, 0.6%	2.1, 1%	6.9	1.8	4.0	
NT2	$E^{\ddagger}$	6.73	5.85	9.06	10.30	−1.74	
	$E^{\ddagger} + \Delta G^{\ddagger}$	22.62			25.63		
	$\Delta\Delta G^{\ddagger}$	7.0, 0%	8.6, 0%	11.1	9.8	12.7	
XT1	$E^{\ddagger}$	5.15	2.1	7.61	3.81	−8.36	
	$E^{\ddagger} + \Delta G^{\ddagger}$	20.43			19.25		
	$\Delta\Delta G^{\ddagger}$	5.4, 0%	4.8, 0%	9.7	3.4	6.1	
XT2	$E^{\ddagger}$	9.36	6.3	11.76	***7.27***[b]	***−4.97***[b]	
	$E^{\ddagger} + \Delta G^{\ddagger}$	24.74			**22.82**		
	$\Delta\Delta G^{\ddagger}$	8.9, 0%	9.0, 0%	13.8	**7.0**, **(7.9)**	***9.5***, ***(8.4)***	

[a] The **5c** rotational isomers are designated as that in Scheme 2. Energies are in kcal·mol^{-1}. Also given are the kinetic product percentage distributions. [b] We failed to optimize the **XT2 5c**(h) H-over-OH···O diasteroisomeric transition structure at the MP2/6-31G(d,p) level for steric reasons, resulting in the TS collapsing to the favored CH_3-over-OH···O structure instead; see the leftmost entries on the same row. **CPD**: $E = -193.47326$ au, $E + \Delta Z = -193.37900$ au, $E + \Delta G = -193.40562$ au at 0° C, MP2/6-31G(d,p); $E = -193.54102$, MP2/6-311+G(2d,p). **5c**: $E = -423.12082$, $E + \Delta G = -422.97208$. **5c**(m): $E = -423.11945$, $E + \Delta G = -422.96891$. **5c**(h): $E = -423.11740$, $E + \Delta G = -422.96846$ au, MP2/6−31G(d,p), all-cis rotamers. **5c**(trans): $E = -423.11945$, $E + \Delta G = -422.97018$. **5c**(h) (trans): $E = -423.11612$, $E + \Delta G = -422.97018$ au.

are about the limits of feasibility with regard to required computational resources.

Solvent Effects on Stereoselectivity and the Mechanism of Hydroxyalkyl Vinyl Ketone Addition to CPD. B3LYP/6-311G(d,p) calculations of **CPD** addition to **5c** within the CPCM model are presented in Table 1 and Figure 1. The comparison between gas-phase and solvent lengths of forming C···C bonds indicates increased reaction asynchronicity even at the low toluene polarity, Figure 1. The geometry changes from the gas-phase to optimized CPCM/B3LYP TSs in nonpolar toluene are minor. In other words, account for the solvent brings no drastic changes of forming C−C bond lengths in terms of concertedness of the addition mechanism. Accounting for the solvent at the 6-311+G(2d,p) basis set level shows some improvement of endo/exo selectivity with respect to gas-phase calculations. The **NC2** − **XC2** TS activation-free-energy difference $\Delta G^{\ddagger}$ is 0.54 kcal·mol^{-1} in the gas phase and 0.78 kcal·mol^{-1} in toluene solution, corresponding to selectivities of 2.5/1 and 3.7/1, respectively, Table 1.

Account for the solvent effect by single-point CPCM/MP2/6-311G(d,p) calculations at the MP2/6-31G(d,p) geometries does not change significantly the endo/exo selectivity of **5c** relative to the gas-phase calculations, deteriorating slightly the **NC2**/**XC2** ratio from 5.5/1 to ∼3.8/1. Thus, solvent effects of nonpolar toluene are apparently negligible within the correlated MP2 MO model. This result confirms the recent conclusion that solvent effects in low-polarity media merely bring additional fine-tuning to predicted computational DA stereoselectivities.[13,20]

In summary, reported MP2 and DFT CPCM calculations indicate that solvent effects on the studied DA addition of 1-*S*-hydroxyalkyl vinyl ketones to cyclopentadiene are relatively small. As a matter of fact, typical polar solvents, for example, alcohols, acetonitrile, DMSO, and so forth, are nucleophilic and would compete for the proton-donating hydroxyl group of present reagent **5** by effectively destroying the internal hydrogen bond, that is, they are unusable in the studied reaction, steered by the O−H···O═C hydrogen bond. In addition, catalysis by the mild Lewis acid H^+ would be completely abolished.

Hybrid QM/QM ONIOM Calculations. The relatively disappointing behavior of DFT calculations for DA selectivity, in particular endo/exo,[11,14,15] selectivity, as well as the heavy computational demands of full-size MP2 calculations even at the low 6-31G(d,p) basis set level prompted us to explore a hybrid approach, ONIOM,[16–18] whereby the [4 + 2]-cycloaddition reaction site is treated at a correlated level of ab initio theory for optimal account of its electronic features. To maintain or even enhance the quality of present calculations, this high QM level would require at least MP2/6-31G(d,p), while the rest of the dienophile can be included in a significantly less demanding HF/6-31G(d) level layer. HF calculations can be deemed sufficient to account for the remote structural effects on asymmetric induction at least on the basis of the observation that the introduced basis set superposition errors, BSSE, are lowest at this level of theory compared to either DFT or MP2.[38–40] Low BSSE should potentially mean more reliable conformations of residues surrounding the DA reaction site.[39] In addition, in the specific case of **5** and **CPD**, we expect that appropriate variations in the choice of ONIOM layers within the dienophiles would provide significant data for the assessment of the role of various possible structural effects in the asym-

TABLE 4: Calculated MP2/6-31G(d,p) Activation (Total Electronic $\Delta E^{\ddagger}$, $\Delta E^{\ddagger} + \Delta ZPE^{\ddagger}$, and $\Delta E^{\ddagger} + \Delta\Delta G^{\ddagger}$) Energies for the Addition of 5b and the Two More Stable (*s-cis*) CH_2-Staggered-over-OH···O(=C) 5a and H-Staggered-over-OH···O(=C) 5a(h) Conformers to CPD in the Gas Phase, kcal·mol^{-1}[a]

		Dienophile 5b	5a	5a(h)
		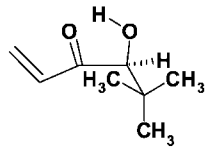	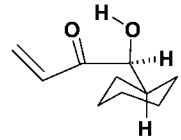	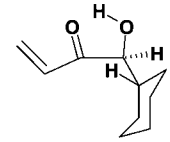
TS				
NC1	$\Delta E^{\ddagger}$	3.14	1.91	4.65
	$\Delta E^{\ddagger}+\Delta\Delta G^{\ddagger}$	19.15	17.9	20.66
	$\Delta\Delta G^{\ddagger}$	4.22 <0.1%	2.1 2.4% (2.1%)	4.87
NC2	$\Delta E^{\ddagger}$	-0.67	0.51	1.45
	$\Delta E^{\ddagger}+\Delta\Delta G^{\ddagger}$	14.93	15.79	17.10
	$\Delta\Delta G^{\ddagger}$	0.0 82.4%	0.0 78.5% (70.3%)	1.31 (7.9%)
XC1	$\Delta E^{\ddagger}$	3.18	1.98	4.68
	$\Delta E^{\ddagger}+\Delta\Delta G^{\ddagger}$	19.26	18.25	20.87
	$\Delta\Delta G^{\ddagger}$	4.33 <0.1%	2.46 1.3% (1.2%)	5.1
XC2	$\Delta E^{\ddagger}$	0.19	1.20	2.01
	$\Delta E^{\ddagger}+\Delta\Delta G^{\ddagger}$	15.86	16.68	17.82
	$\Delta\Delta G^{\ddagger}$	0.93 17.5%	0.89 17.8% (16%)	2.0 (2.5%)
Dienophile	MP2=	-462.3049909	-539.4869845	-539.4834367
	E+ZPE	-462.091631	-539.234589	-539.231003
	E + ΔG	-462.128170	-539.273038	-539.269400
CPD	MP2=	-193.4732618		
	E+ZPE	-193.378995		
	E + ΔG	-193.405619		

[a] For each entry, the respective kinetic product percentage contribution is given also. In parentheses are percentages of **5a**, calculated with account for the minor rotational isomer.

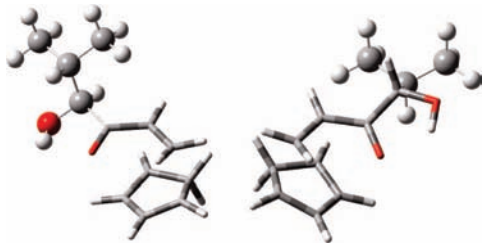

Figure 3. Two ONIOM layer selections for **5c** with the intramolecular hydrogen bond in the low layer, left, and in the high layer, right. The high MP2/6-31G(d,p) level layer is depicted with tubes and the low HF/6-31G(d) level layer with balls.

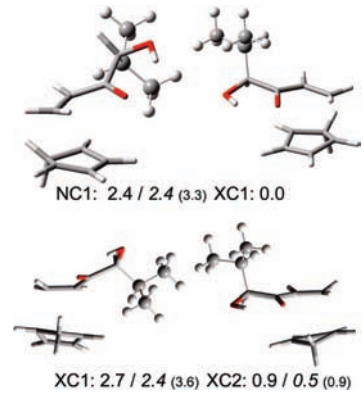

Figure 4. ONIOM(MP2/6-31G(d,p):HF/6-31G(d)) TSs for the reaction of *s-cis* **5c** and **CPD**. For comparison, relative activation free energies in kcal·mol^{-1} are shown for the complete MP2/6-31G(d,p), regular type, B3LYP/6−311+G(2d,p), italic, and for the ONIOM (petite) calculations.

metric induction. The choice of ONIOM is additionally favored by negligible effects of low-polarity solvents used in the experiment and discussed above.

Our initial ONIOM separation of the reacting system includes only the "generic" [4 + 2]-cycloaddition site into the high-level layer, leaving the chiral carbon atom and thus also the intramolecular hydrogen bond in the low-level layer, Figure 3, left. We note at first that the optimized transition structures at this ONIOM separation still retain the cyclic hydrogen-bonding arrangement. Thus, with this selection of layers, only the hydrogen bond energy is deliberately underestimated, and the possible role of hydrogen bonding in the chiral dienophile molecule is largely neglected. The described ONIOM separation experiment has a strong effect on the resulting computational prediction of stereoselectivity. Diastereoface selectivity for the reaction of **5c** and **CPD** is increased to practically 100%,[2] while endo/exo selectivity is reduced relative to the full MP2/6-31G(d,p) value to 0.5, which is worse even than the B3LYP/6-311+G(2d,p) result. Therefore, we try another ONIOM separation, including the hydroxyalkyl group with the chiral carbon, hence the intramolecular hydrogen bond, into the MP2/6-31G(d,p) layer and leaving in the low-level HF/6-31G(d) layer only the bulky alkyl substituent, Figure 3, right.

Figure 4 gives a comparison of relative activation free energies with respect to the favored diastereoisomer, **NC2**, between the complete MP2/6-31G(d,p) model and the second ONIOM selection. With regard to cycloaddition stereoselectivities, the latter ONIOM results are satisfactory; while comparing favorably to the complete MP2 calculations in terms of required computational resources, ONIOM calculations with

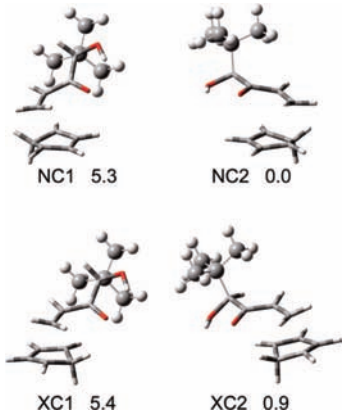

Figure 5. ONIOM(MP2/6-31G(d,p):HF/6-31G(d)) transition structures for the reaction of *s-cis* **5b** and **CPD**. Relative activation free energies are given in kcal·mol^{-1} with respect to the favored **NC2** (*S*,*S*)-isomer.

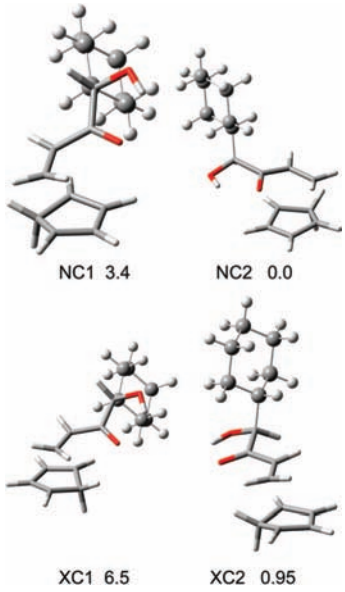

Figure 6. ONIOM(MP2/6-311G(d,p):HF/6-31G(d)) transition structures for the reaction of *s-cis* **5a** and **CPD**. Relative free activation energies from single-point ONIOM(CCSD/6-311G(d,p):HF/6-31G(d)) with respect to the favored **NC2** isomer are in kcal·mol^{-1}.

MP2 in the high layer are preferable to the best B3LYP results in terms of the quality of stereoselectivity predictions, ~4.5/1 endo/exo, and higher than 100/1 (*SS* + *RS*, or **II**)/(*RR* + *SR*, or **I**). Therefore, we pursue further the Diels−Alder addition stereoselectivities of dienophiles **5** to **CPD** using the second ONIOM layer definition.

Present ONIOM calculations on the reaction of *s-trans* **5c** with cyclopentadiene show again, after the full MP2/6-31G(d,p) results above, that this isomer practically does not participate in the cycloaddition, in line with the conclusions on the basis of experimental studies of this reaction[2] and those reached also in other asymmetric DA reactions by experiment[12] and computations.[11] Hereafter, we discuss the results from the computational modeling of DA additions of **5a** and **5b** to **CPD** for the corresponding *s-cis* dienophiles only.

ONIOM (MP2/6-31G(d,p):HF/6-31G(d)) calculations for the DA addition of **5b** to **CPD** predict the same endo/exo and some increase of diastereoface selectivity relative to **5c**, Figure 5; compare Figure 4. Experimentally, **5b** is the ketol showing the highest selectivity among the studied methyl vinyl ketone derivatives, up to 8/1 endo/exo, and 100/1 π diastereoface *SS*/*RR* selectivity.[2] The calculated relative ONIOM activation free energies for this reaction somewhat underestimate the endo/exo selectivity, giving a value of ~4.5/1, and somewhat overestimate diastereoselectivity by predicting ~0.01% of the (*R*,*R*)-diastereoisomers. The latter results are only qualitatively correct, while their quantitative precision is still below satisfactory.

Our ONIOM (MP2/6-31G(d,p):HF/6-31G(d)) results for the DA reaction of **5a** and **CPD**, Figure 6, show high diastereoselectivity *SS*/*RR*, in agreement with experimental data.[2] The qualitative prediction of endo/exo selectivity with the large cyclohexyl substituent shows once again the correct trend, indicating a 4.9/1 preference for the endo (*S*,*S*)-diastereoisomer over the exo (*S*,*R*) one, in good qualitative accord with the experimental 8/1 endo/exo ratio.[2] Note for comparison that B3LYP/6-311+G(2d,p) calculations for the same reaction of **5a** and **CPD** predict only a minimal endo/exo selectivity of ~2.5/1 or less, that is, at this level of DFT, the *SS* is favored over the *RR s-cis* diastereoisomeric TS by an energy difference of less than 0.2 kcal·mol^{-1}, with a free-energy difference of less than 0.5 kcal·mol^{-1}. At a lower, for example, 6-31G(d) level of B3LYP calculations, the predicted endo/exo preference vanishes or is even inverted.

As indicated in Table 3, higher basis set MP2/6-311+G(2d,p) calculations predict somewhat higher endo/exo as well as diastereoface selectivities. Therefore, we additionally refine our ONIOM calculations by geometry optimizations at the MP2/6-311G(d,p):HF/6-31G(d) level. We keep the same separation of layers, with the high MP2 layer including essential fragments as the cycloaddition reaction site, the chiral carbon, and the hydrogen-bonded fragment. The low HF layer again includes only the hydrocarbon fragment. The results for the addition of most stable *s-cis* dienophile **5a**−**c** conformers to **CPD** are listed in Table 5. The calculations predict **5a** and the model **5c** to have practically equal endo/exo selectivities of ~4.5/1, while **5b** has higher selectivity, in line with experiments. The **si**-diastereofacial attack of the diene on the dienophile is preferred, with predicted values for the **NC2/NC1** ratio of ~240/1 for the endo and those for **XC2/XC1** of ~50/1 for the exo attack on all dienophiles **5** studied, somewhat higher than the fully optimized MP2/6-31G(d,p) results shown in Table 3. Further ONIOM improvement to single-point ONIOM(CCSD/6-311G(d,p):HF/6-31G(d))//ONIOM(MP2/6-311G(d,p):HF/6-31G(d)) brings endo/exo selectivity to ~8/1 for **5a** and **5c** and to more than 10/1 in the case of **5b** addition to **CPD**, in good agreement with experiment,[2] Table 5.

As discussed earlier, the carried ONIOM calculations consistently indicate that exclusion of the hydrogen bond from the high-level layer is deleterious to the stereochemical predictions, thus corroborating the experimentally deduced importance of the hydrogen bond as an essential link between the chiral carbon and the cycloaddition reaction site. The explicit account for electron correlation in the cycloaddition reaction site is essential for the qualitatively correct prediction of prevailing endo over exo selectivity, even though the use of MP2 may be insufficient and possibly a source of undesired errors in quantitative terms. As shown here, proper account for correlation effects in the reaction site by CCSD gives quantitatively correct predictions of DA stereoselectivities.

Are DFT calculations a better alternative than ONIOM? Apart from the known tendency of B3LYP to give wrong predictions for endo/exo selectivity in Diels−Alder additions,,[39] we bring another argument in favor of calculations taking account for dynamic electron correlation effects in the course of geometry optimizations, an alias during the search for stationary points

TABLE 5: Activation Energies, Absolute and Relative TS Activation Free Energies from Optimized ONIOM(MP2/6-311G(d,p):HF/6-31G(d)) O-MP2 Calculations for the CPD Addition to 5a, 5b, and 5c (Most Stable CH_2-over-OH···O Conformers of 5a and 5c) and from Single-Point ONIOM (CCSD/6-311G(d,p):HF/6-31G(d))//ONIOM(MP2/6-311G(d,p):HF/6-31G(d)) O-CCSD Calculations[a]

		5a		5b		5c	
TS	dienophile	O-MP2	O-CCSD	O-MP2	O-CCSD	O-MP2	O-CCSD
NC1	$\Delta E^{\ddagger}$	1.86	16.03	24.20	41.24	1.77	15.93
	$\Delta E^{\ddagger} + \Delta\Delta G^{\ddagger}$	39.93		63.18		39.83	
	$\Delta\Delta G^{\ddagger}$	3.4, 0.3%	2.5, 1.3%	4.7, −	3.5, 0.3%	3.3, 0.3%	2.4, 1.6%
NC2	$\Delta E^{\ddagger}$	−1.46	13.54	19.77	37.30	−1.51	13.49
	$\Delta E^{\ddagger} + \Delta\Delta G^{\ddagger}$	36.57		58.50		36.54	
	$\Delta\Delta G^{\ddagger}$	0.0, 83%	0.0, 87%	0.0, 84%	0.0, 85.7%	0.0, 82.5%	0.0, 86.7%
XC1	$\Delta E^{\ddagger}$	2.00	16.56	24.33	41.59	1.87	16.43
	$\Delta E^{\ddagger} + \Delta\Delta G^{\ddagger}$	40.37		63.44		40.28	
	$\Delta\Delta G^{\ddagger}$	3.8, 0.1%	3.0, 0.6%	4.9, −	3.8, 0.2%	3.7, 0.2%	2.9, 0.7%
XC2	$\Delta E^{\ddagger}$	−0.53	14.78	20.63	38.39	−0.58	14.73
	$\Delta E^{\ddagger} + \Delta\Delta G^{\ddagger}$	37.53		59.49		37.49	
	$\Delta\Delta G^{\ddagger}$	0.96, 17%	1.24, 11%	0.99, 16%	1.09, 13.9%	0.95, 16.9%	1.24, 11%
CPD	MP2 = −193.53622						CCSD = −193.57580
	E + ZPE: −193.47933						
	$E + \Delta G$: −193.50594						
5a	O-MP2: −538.74389						CCSD = −538.78240
	E + ZPE: −538.48533						
	$E + \Delta G$: −538.52382						
5b	O-MP2: −461.82945						CCSD = −461.86805
	E + ZPE: −461.61209						
	$E + \Delta G$: −461.64868						
5c	O-MP2: −422.79926						CCSD = −422.83777
	E + ZPE: −422.61213						
	$E + \Delta G$: −422.64800						

[a] All values are in kcal·mol^{-1}. Product percentage distributions are given next to each entry.

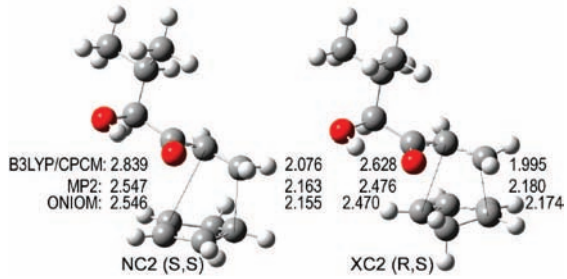

Figure 7. Selected geometry parameters of favored endo and exo Diels−Alder transition structures by the three computational approaches, DFT, MP2, and MP2-ONIOM. Forming bond lengths (thin lines, Å) in DFT have the ratio 1.37 (*S*,*S*), Δd = 0.76 Å, and 1.32 (*R*,*S*), Δd = 0.63 Å, while the values from the two correlated MO methods are 1.18 (*S*,*S*), Δd = 0.38 Å, and 1.14 (*R*,*S*), Δd = 0.30 Å, showing significant bias in DFT preferences in the direction of the stepwise addition mechanism.

on the reaction potential energy surface. For this purpose, we use a comparison between the results of TS searches with the three computational approaches, given in Figure 7. As demonstrated by shown geometry parameters of the same preferred TSs and related to the ultimate criterion, the experiment, DFT B3LYP computations have apparently a stronger tendency for a biradicaloid reaction mechanism than the two MO approaches. MP2 and MP2-ONIOM, on the other hand, tend to favor the concerted "almost synchronous" mechanism. Specifically in the case of present hydroxyalkyl vinyl ketone dienophiles, where catalysis by H^+ of the hydrogen bond, acting as a Lewis acid,[41] brings some additional bias toward a two-step mechanism, MP2-ONIOM results are close to the experimental endo/exo selectivity and thus indicate as correct the "almost synchronous" alternative.[13,42,43] On the other hand, B3LYP potential energy surfaces for the concerted and diradicaloid mechanisms seem closer to one another, as noted, for example, with geometries in Figure 7. Thus, the seemingly computationally convenient approach of single-point MP2 over B3LYP geometries cannot be justified as long as the B3LYP TSs on the reaction PES are far away from the respective MP2 stationary point configurations.[41,42]

Conclusions

Comparisons between the three computational approaches unequivocally support the opinion that endo/exo selectivity of Diels−Alder additions is governed by dynamic electron correlation effects between the interacting diene and dienophile π-electronic systems. Therefore, DFT methods perform miserably with respect to endo/exo selectivity, while they are qualitatively satisfactory with respect to diastereofacial selectivity. Correlated methods perform considerably better in this respect, with MP2 giving approximately twice better endo/exo selectivity. The tested hybrid ONIOM approaches, selected to preserve the largest part of dynamic correlation in the reacting π system, give either comparable selectivies with full MP2 calculations, the O-MP2 approach, or are superior to full MP2, the O-CCSD approach. To our understanding, ONIOM models of Diels−Alder reactions may reliably predict product selectivities, provided that the dynamic electron correlation is properly accounted for.

On the basis of discussed correlated MO MP2 calculations, we conclude that diastereoface selectivities, for example, *SS* against *RR* enantiomers **NC2** versus **NC1** in the case of **5a** and **5b** additions to **CPD**, appear completely determined by steric repulsion factors. Dynamic electron correlation effects within the cycloaddition reaction site dominate in the preference of endo *SS* isomeric products over the corresponding *RS* exo diastereoisomers.

Acknowledgment. Part of this work has been carried out during repeated stays of J.K. at the University of Alcalá, Alcalá de Henares (Madrid), Spain. Support from the Spanish Ministry of Education, Culture and Sport in the form of two Giner de los Rios professorships, as well as computational facilities under projects BQU2003-07281 and CTQ2006–07643, Spain, are gratefully acknowledged. Computing facilities available to the BAS under the EGEE-GRID initiative, started within the VI-th EU Framework program, have also been actively involved in the reported research.

Supporting Information Available: Full ref 21; tables of absolute B3LYP, MP2, and ONIOM energies; full IRC profile for a MP2 reaction model; $\pi-\pi$ stacking complexes, structures, and coordinates; transition structure coordinates; and conformational analyses. This material is available free of charge via the Internet at http://pubs.acs.org.

References and Notes

(1) Helmchen, G.; Karge, R.; Weetman, J. In *Modern Synthetic Methods*; Scheffold, R., Ed.; Springer-Verlag: Berlin, Heidelberg, Germany,1986; Vol. 4, pp 261−306.

(2) Choy, W.; Reed, L. A.; Masamune, S. *J. Org. Chem.* **1983**, *48*, 1137–1139.

(3) Masamune, S.; Reed, L. A.; Davis, J. T.; Choy, W. *J. Org. Chem.* **1983**, *48*, 4441–4444.

(4) Coxon, J. M.; Froese, R. D. J.; Ganguly, B.; Marchand, A. P.; Morokuma, K. *Synlett* **1999**, 1681–1703.

(5) (a) Lipkowitz, K. B.; Pradhan, M. *J. Org. Chem.* **2003**, *68*, 4648–4656. (b) Lipkowitz, K. B.; D'Hue, C. A.; Sakamoto, T.; Stack, J. N. *J. Am. Chem. Soc.* **2002**, *124*, 14255–14267.

(6) Evans, D. A.; Johnson, D. S. In *Comprehensive Asymmetric Catalysis I-III*; Jacobsen, E. N., Pfaltz, A., Yamamoto, H., Eds. Springer Verlag: Berlin, Heidelberg, 1999; p 1178.

(7) Wiest, O.; Montiel, D. C.; Houk, K. N. *J. Phys. Chem. A* **1997**, *101*, 8378–8388, and references therein.

(8) Kong, S.; Evanseck, J. D. *J. Am. Chem. Soc.* **2000**, *122*, 10418–10427, and references therein.

(9) (a) Montgomery, J. A.; Frisch, M. J.; Ochterski, J. W.; Peterson, G. A. *J. Chem. Phys.* **1999**, *110*, 2822–2827. (b) Montgomery, J. A.; Frisch, M. J.; Ochterski, J. W.; Peterson, G. A. *J. Chem. Phys.* **2000**, *112*, 6523–6542.

(10) Guner, V.; Khuong, K. S.; Leach, A. G.; Lee, P. S.; Bartberger, M. D.; Houk, K. N. *J. Phys. Chem. A* **2003**, *107*, 11445–11459.

(11) Bakalova, S. M.; Santos, A. G. *J. Org. Chem.* **2004**, *69*, 8475–8481.

(12) (a) Poll, T.; Helmchen, G.; Bauer, P. *Tetrahedron Lett.* **1984**, *25*, 2191–2194. (b) Poll, T. PhD Dissertation, Universität Würzburg, 1988.

(13) Rulisek, L.; Sebek, P.; Havlas, Z.; Hrabal, R.; Capek, P.; Svatos, A. *J. Org. Chem.* **2005**, *70*, 6295–6302.

(14) (a) Besler, B. H.; Merz, K. M., Jr.; Kollman, P. A. *J. Comput. Chem.* **1990**, *11*, 431–439. (b) Singh, U. C.; Kollman, P. A. *J. Comput. Chem.* **1984**, *5*, 129–145.

(15) Garcia, J. I.; Mayoral, J. A.; Salvatella, L. *Acc. Chem. Res.* **2000**, *33*, 658–664.

(16) (a) Humbel, S.; Sieber, S.; Morokuma, K. *J. Chem. Phys.* **1996**, *105*, 1959–1967. (b) Svensson, M.; Humbel, S.; Froese, R. D. J.; Matsubara, T.; Sieber, S.; Morokuma, K. *J. Phys. Chem.* **1996**, *100*, 19357–19363.

(17) Dudding, T.; Houk, K. N. *Proc. Natl. Acad. Sci. U.S.A.* **2004**, *101*, 5770–5775.

(18) Deng, W.; Vreven, T.; Frisch, M. J.; Wiberg, K. B. *J. Mol. Struct.: THEOCHEM* **2006**, *775*, 93–99.

(19) Jorgensen, W. L.; Lim, D.; Blake, J. F. *J. Am. Chem. Soc.* **1993**, *115*, 2936–2942.

(20) Acevedo, O.; Jorgensen, W. L. *J. Chem. Theory Comput.* **2007**, *3*, 1412–1419.

(21) Frisch, M. J. Trucks, G. W.; Schlegel, H. B.; Scuseria, G. E.; Robb, M. A.; Cheeseman, J. R.; Montgomery, J. A., Jr.; Vreven, T.; Kudin, K. N.; Burant, J. C.; Millam, J. M.; Iyengar, S. S.; Tomasi, J.; Barone, V.; Mennucci, B.; Cossi, M.; Scalmani, G.; Rega, N.; Petersson, G. A.; Nakatsuji, H.; Hada, M.; Ehara, M.; Toyota, K.; Fukuda, R.; Hasegawa, J.; Ishida, M.; Nakajima, T.; Honda, Y.; Kitao, O.; Nakai, H.; Klene, M.; Li, X.; Knox, J. E.; Hratchian, H. P.; Cross, J. B.; Bakken, V.; Adamo, C.; Jaramillo, J.; Gomperts, R.; Stratmann, R. E.; Yazyev, O.; Austin, A. J.; Cammi, R.; Pomelli, C.; Ochterski, J. W.; Ayala, P. Y.; Morokuma, K.; Voth, G. A.; Salvador, P.; Dannenberg, J. J.; Zakrzewski, V. G.; Dapprich, S.; Daniels, A. D.; Strain, M. C.; Farkas, O.; Malick, D. K.; Rabuck, A. D.; Raghavachari, K.; Foresman, J. B.; Ortiz, J. V.; Cui, Q.; Baboul, A. G.; Clifford, S.; Cioslowski, J.; Stefanov, B. B.; Liu, G.; Liashenko, A.; Piskorz, P.; Komaromi, I.; Martin, R. L.; Fox, D. J.; Keith, T.; Al-Laham, M. A.; Peng, C. Y.; Nanayakkara, A.; Challacombe, M.; Gill, P. M. W.; Johnson, B.; Chen, W.; Wong, M. W.; Gonzalez, C.; Pople, J. A. *Gaussian 03*, revision C.02; Gaussian, Inc.: Wallingford, CT, 2004.

(22) Hehre, W. J.; Radom. L.; Schleyer, P. v. R.; Pople, J. A. *Ab initio MO Theory*; Wiley: New York, 1986.

(23) (a) Gonzales, C.; Schlegel, H. B. *J. Chem. Phys.* **1989**, *90*, 2154–2161. (b) Shaik, S. S.; Schlegel. H. B.; Wolfe, S. *The SN 2 Mechanism*; Wiley: New York, 1992.

(24) Schmidt, M. W.; Baldridge, K. K.; Boatz, J. A.; Elbert, S. T.; Gordon, M. S.; Jensen, J. J.; Koseki, S.; Matsunaga, N.; Nguyen, K. A.; Su, S.; Windus, T. L.; Dupuis, M.; Montgomery, J. A. *J. Comput. Chem.* **1993**, *14*, 1347–1363.

(25) (a) Dapprich, S.; Komaromi, I.; Byun, K. S.; Morokuma, K.; Frisch, M. J. *J. Mol. Struct.: THEOCHEM* **1999**, *461−462*, 1–21. (b) Froese, R. D. J.; Morokuma, K. In *Encylopedia of Computational Chemistry*; Schleyer, P. v. R. , Ed.; John Wiley and Sons: Chichester, Sussex, U.K., 1998; Vol. 2, pp 1244−1257.

(26) (a) Cizek, J. *Adv. Chem. Phys.* **1969**, *14*, 35. (b) Pople, J. A.; Krishnan, R.; Schlegel, H. B.; Binkley, J. S. *Int. J. Quantum Chem.* **1978**, *14*, 545–560. (c) Purvis, G. D.; Bartlett, R. J. *J. Chem. Phys.* **1982**, *76*, 1910–1918. (d) Crawford, T. D.; Schaefer III, H. F., In *Review of Computational Chemistry*; Lipkowitz, K. B., Boyd, D. B., Eds.; 2000; Vol. 14, pp 33−136.

(27) Tomasi, J.; Persico, M. *Chem. Rev.* **1994**, *94*, 2027–2094.

(28) (a) Klamt, A.; Schüürmann, G. *J. Chem. Soc., Perkin Trans. 2* **1993**, 799–806. (b) Klamt, A.; Jonas, V.; Buerger, T.; Lohrenz, J. C. W. *J. Phys. Chem. A* **1998**, *102*, 5074–5085.

(29) Rowley, D.; Steiner, H. *Discuss. Faraday Soc.* **1951**, *27*, 5299–5306.

(30) Acevedo, O.; Evanseck, J. D. *Org. Lett.* **2003**, *5*, 649–652.

(31) (a) Maskill, H. *The Physical Basis of Organic Chemistry*; Oxford University Press: New York, 1985, pp 293. (b) Zefirov, N. S. *Tetrahedron* **1977**, *33*, 2719–2722.

(32) White, J. D.; Demnitz, F. W. J.; Oda, H.; Hassler, C.; Snyder, J. P. *Org. Lett.* **2000**, *2*, 3313–3316.

(33) Loncharich, R. J.; Schwartz, T. R.; Houk, K. N. *J. Am. Chem. Soc.* **1987**, *109*, 14–23.

(34) Durig, J. R.; Little, T. S. *J. Chem. Phys.* **1981**, *75*, 3660–3668.

(35) (a) Prelog, V. *Helv. Chim. Acta* **1953**, *36*, 308–319. (b) Prelog, V.; Tsatsas, G. *Helv. Chim. Acta* **1953**, *36*, 1178–1180.

(36) Cram, D. J.; Abd Elhafez, F. A. *J. Am. Chem. Soc.* **1952**, *74*, 5828–5835.

(37) Walborsky, H. M.; Barash, L.; Davis, T. C. *Tetrahedron* **1963**, *19*, 2333–2351.

(38) Boys, S. F.; Bernardi, F. *Mol. Phys.* **1970**, *19*, 553–566.

(39) van Mourik, T.; Karamertzanis, P. G.; Price, S. L. *J. Phys. Chem. A* **2006**, *110*, 8–12.

(40) Johnson, E. R.; Di Labio, G. A. *Chem. Phys. Lett.* **2006**, *419*, 333–339.

(41) Chandrasekhar, J.; Shariffskul, S.; Jorgensen, W. L. *J. Phys. Chem. B* **2002**, *106*, 8078–8085.

(42) Jones, G. A.; Paddon-Row, M. N.; Sherburn, M. S.; Turner, C. I. *Org. Lett.* **2002**, *4*, 3789–3792.

(43) Bakalova, S. M.; Santos, A. G. *Eur. J. Org. Chem.* **2006**, 1779–1789.

JP803701Y